

### **LETTER • OPEN ACCESS**

# A first proof of knot localization for polymers in a nanochannel

To cite this article: Nicholas R Beaton et al 2024 J. Phys. A: Math. Theor. 57 38LT01

View the article online for updates and enhancements.

### You may also like

- The role of mobility in epidemics near criticality
  Beatrice Nettuno, Davide Toffenetti,
  Christoph Metzl et al.
- A generalized dynamic asymmetric exclusion process: orthogonal dualities and degenerations
   Wolter Groenevelt and Carel Wagenaar
- On gauge Poisson brackets with prescribed symmetry M Avendaño-Camacho, J C Ruíz-Pantaleón and Yu Vorobiev



J. Phys. A: Math. Theor. 57 (2024) 38LT01 (14pp)

https://doi.org/10.1088/1751-8121/ad6c01

Letter

### A first proof of knot localization for polymers in a nanochannel

Nicholas R Beaton<sup>1</sup>, Kai Ishihara<sup>2</sup>, Mahshid Atapour<sup>3</sup>, Jeremy W Eng<sup>4,8</sup>, Mariel Vazquez<sup>5,6</sup>, Koya Shimokawa<sup>7</sup> and Christine E Soteros<sup>4,\*</sup>

- <sup>1</sup> School of Mathematics and Statistics, University of Melbourne, Melbourne 3010,
- <sup>2</sup> Department of Mathematics, Hiroshima University, Higashi-Hiroshima 739-8526,
- <sup>3</sup> Mathematics and Statistics, Capilano University, North Vancouver V7J 3H5, Canada
- <sup>4</sup> Department of Mathematics and Statistics, University of Saskatchewan, Saskatoon S7N 5E6, Canada
- <sup>5</sup> Department of Microbiology and Molecular Genetics, University of California Davis, Davis, CA 95616, United States of America
- <sup>6</sup> Department of Mathematics, University of California Davis, Davis, CA 95616, United States of America
- <sup>7</sup> Department of Mathematics, Ochanomizu University, Tokyo 112-8610, Japan

E-mail: soteros@math.usask.ca

Received 3 May 2024; revised 19 July 2024 Accepted for publication 6 August 2024 Published 30 August 2024



### **Abstract**

Based on polymer scaling theory and numerical evidence, Orlandini, Tesi, Janse van Rensburg and Whittington conjectured in 1996 that the limiting entropy of knot-type K lattice polygons is the same as that for unknot polygons, and that the entropic critical exponent increases by one for each prime knot in the knot decomposition of K. This Knot Entropy (KE) conjecture is consistent with the idea that for unconfined polymers, knots occur in a localized way (the knotted part is relatively small compared to polymer length). For full confinement (to a sphere or box), numerical evidence suggests that knots are much less localized. Numerical evidence for nanochannel or tube confinement is mixed, depending

Original Content from this work may be used under the terms of the Creative Commons Attribution 4.0 licence. Any further distribution of this work must maintain attribution to the author(s) and the title of the work, journal citation and DOI.

<sup>(</sup>currently) Sask Polytech, Saskatoon S7K 0R8, Canada.

Author to whom any correspondence should be addressed.



on how the size of a knot is measured. Here we outline the proof that the KE conjecture holds for polygons in the  $\infty \times 2 \times 1$  lattice tube and show that knotting is localized when a connected-sum measure of knot size is used. Similar results are established for linked polygons. This is the first model for which the knot entropy conjecture has been proved.

Keywords: lattice polymer, knot localization, self-avoiding polygon, lattice link, DNA topology, lattice tube, nanochannel

#### 1. Introduction

Interest in knotting and linking in ring polymers dates back to at least the 1930s, when geneticists Navashin and McClintock observed circular chromosomes linked by DNA replication [32, 35]. In 1962, Frisch and Wasserman [25] and Delbrück and Fuller [17] conjectured that sufficiently long ring polymers in dilute solution are knotted with high probability. The first proof of the Frisch–Wasserman–Delbrück (FWD) conjecture was for a lattice polygon model of ring polymers [40, 51]. The conjecture was later proved for a number of off-lattice polymer models [19–21, 29]. More recently, the probability of knotting has been explored for models of knot diagrams [13, 24, 55].

With the FWD conjecture proved, interest turned to studying the statistics for specific knottypes. Studies of statistics of knotted polygons and entropic arguments [37] have led polymer physicists to believe that the most likely configurations have the knotted components highly localized in the chain [39], somewhat like pearls on a long string. In the simple cubic lattice, where polygons have vertices in  $\mathbb{Z}^3$  and edges of unit length, studying knot entropy involves studying the number  $p_n(K)$  of n-edge polygons with fixed knot-type K and its dependence on K as  $n \to \infty$ . From the knot localization hypothesis, polymer scaling theory and numerical evidence, Orlandini, Tesi, Janse van Rensburg and Whittington stated the following 1996 Knot Entropy (KE) conjecture for lattice polygons.

**Knot Entropy Conjecture ([36, 37]).** For any given knot-type K, as  $n \to \infty$ ,  $p_n(K)$  satisfies the asymptotic equation

$$p_n(K) = B_K n^{f_K} p_n(0_1) (1 + o(1)), \tag{1}$$

where  $0_1$  is the unknot,  $f_K$  denotes the number of prime knot factors in the knot decomposition of K and  $f_{0_1} \equiv 0$ . Moreover,

$$p_n(0_1) = A_{0_1} n^{\alpha_{0_1}} \mu_{0_1}^n (1 + o(1)), \tag{2}$$

where  $\alpha_{0_1}$  is called the **unknot entropic critical exponent** and  $\mu_{0_1}$  is called the **unknot exponential growth constant**.  $\kappa_{0_1} = \log \mu_{0_1}$  is the limiting entropy per monomer for the unknot and is also called the **unknot growth rate**.  $B_K$ ,  $A_{0_1}$  and  $\mu_{0_1}$  are potentially lattice-dependent.

Despite strong numerical evidence in support of this conjecture [37, 42], very little has been proved analytically. For the simple cubic lattice  $\mathbb{Z}^3$ , it is known that the limit defining  $\mu_{0_1}$  exists and that  $\mu_{0_1} < \mu$  [51], where  $\mu$  denotes the exponential growth constant for all n-edge self-avoiding lattice polygons, regardless of knot-type. However existence of  $\alpha_{0_1}$  and of exponential growth constants for  $K \neq 0_1$  remain open problems. Establishing the validity of the KE Conjecture, along with a result similar to (2) for *all* n-edge polygons regardless of knot-type, would imply that the probability of a random n-edge polygon having knot-type K scales with n like  $C_K(\frac{\mu_{0_1}}{\mu})^n n^{\sigma + f_K}$ , for  $\sigma$  independent of K.



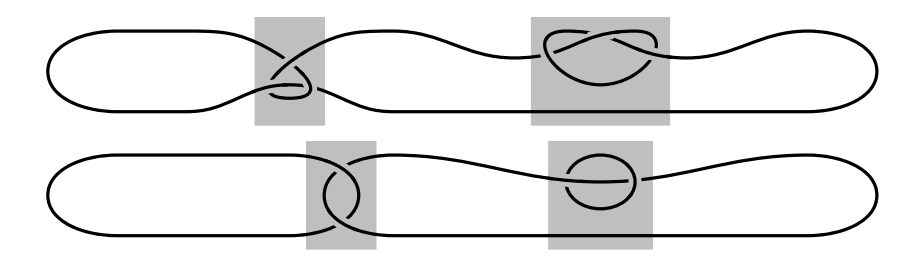


**Figure 1.** Top: a schematic of a typical long narrow polygon with knot-type  $3_1 \# 3_1$ . Bottom: a schematic of a connected sum of two Hopf links. In each, the 'knotted parts' or 'linked parts' (shaded) are highly localized compared to the length (or span) of the whole embedding.

Experiments of DNA packing or DNA in nanochannels have motivated interest in the knot and link statistics of polymers under confinement [2, 41]. Confinement conditions which have been modelled include: 'full' confinement as in a sphere or capsid; restricting only two directions as in a nanochannel or tube; and restricting only one direction as in a slab [33, 38]. Numerical evidence for spherical confinement suggests that knots are much less localized than for unconfined polymers [18]. However, an off-lattice study for tube confinement [34] at small tube diameters was less conclusive. The occurrence of factors in composite knots followed a Poisson distribution, consistent with the knot probability scaling form  $C_K(\frac{\mu_{0_1}}{...})^n n^{\sigma + f_K}$  and with knot localization, however large knot-sizes measured by arc-length appeared inconsistent with knot localization. Recent lattice tube results for a connected-sum measure of knot-size show however that the arc-length results of [34] are consistent with knot localization [6] (see figure 1 for a schematic). Numerical studies of the lattice tube model also led to the supposition that the KE Conjecture holds for lattice tube polygons [8]. In this letter we give an outline of our recent proof of the KE Conjecture for the smallest tube that admits non-trivial knots; the full details of the proof are available at [9] and will be published separately. Here, we aim to highlight the general ingredients of the proof and its consequences.

Lattice tube models have proved to be useful for modelling polymers under confinement since the 1970s [27, 54]. We focus on tubular sublattices of the simple cubic lattice. These have been studied previously in various contexts [1, 3–8, 22, 44, 45, 48]. Unless stated otherwise, the notation and definitions used here are as in [7]. For positive integers  $M_1, M_2$ , the semi-infinite sublattice of  $\mathbb{Z}^3$  induced by the vertex set  $\{(x,y,z) \in \mathbb{Z}^3 : x \ge 0, 0 \le y \le M_1, 0 \le z \le M_2\}$  is called the  $M_1 \times M_2$  tube and denoted by  $\mathbb{T}_{M_1,M_2} \equiv \mathbb{T}$ .

We are interested in embeddings of simple closed curves, *lattice links*, in  $\mathbb{T}$  and restrict to those which occupy at least one edge in the plane x=0. A lattice polygon or *lattice knot* is a one component lattice link. We define  $p_{\mathbb{T},n}(L)$  to be the number of n-edge embeddings of a non-split link type L in  $\mathbb{T}$ . We do not consider split links L, i.e. two or more separable simple closed curves, since their n-edge embedding counts are not finite. For general  $\mathbb{T}$ , little is known about  $p_{\mathbb{T},n}(L)$  when  $L \neq 0_1$ . However, in [28] there is a characterization of the link types for which  $p_{\mathbb{T},n}(L) > 0$  for some n and it is shown that  $\mathbb{T}^* = \mathbb{T}_{2,1}$  is the smallest tube that admits non-trivial links. The links in  $\mathbb{T}^*$  are all 4-plats or connected sums of 4-plats. Figure 2(A) illustrates a knotted polygon in  $\mathbb{T}^*$ . Even though  $\mathbb{T}^*$  is narrow, polygons in  $\mathbb{T}^*$  are physically relevant for modelling DNA in nanochannels.  $\mathbb{T}^*$ 's dimensions  $(2 \times 1)$  are on the same order as a polygon's Kuhn length [6, 8] and thus comparable to channel sizes in DNA experiments [16]. Importantly all prime knots with 7 or fewer crossings and the majority for up to 9 crossings



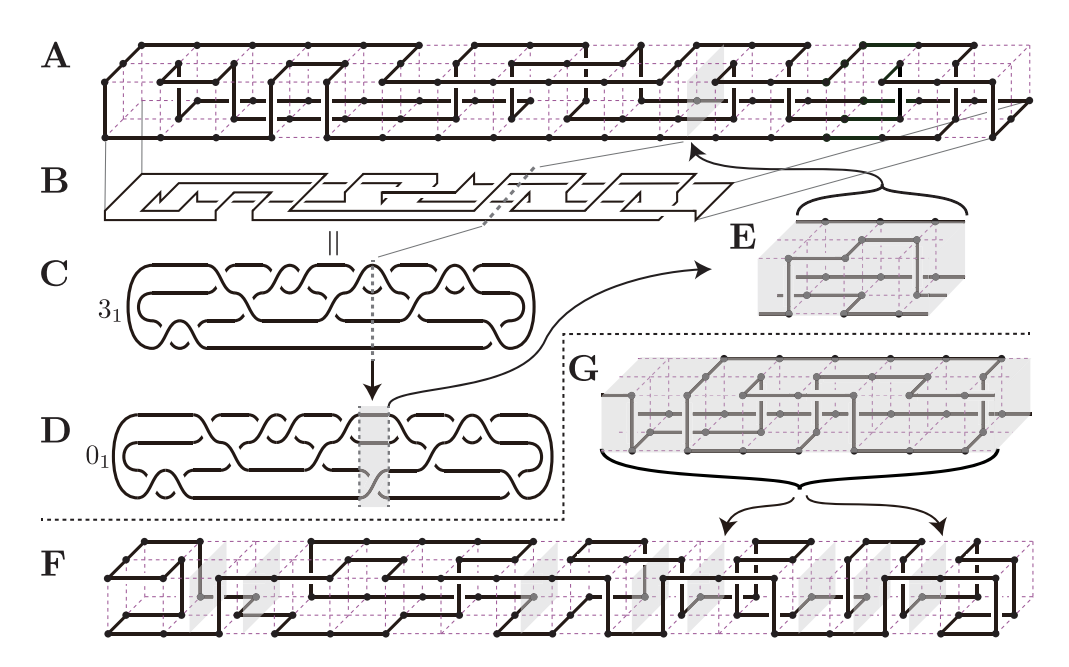


Figure 2. (A) Upper bound example. A 98-edge polygon of knot-type  $3_1$  (trefoil) in  $\mathbb{T}^*$ . The insert (E) enclosed in a 3-block is a 4-braid containing a half twist of 2 strings. When inserted in (A) at the identified location, the 3-block converts the  $3_1$  into an unknot. (B) A shifted knot diagram obtained from a 2-dimensional projection of the polygon in (A). (C) The 4-plat diagram associated with the  $3_1$  polygon in (A). (D) A 4-plat diagram of an unknot obtained by inserting a half twist at the location indicated with a dotted line in (B) and in (C). (E) A lattice tube embedding of the corresponding half twist from (D). (F) Lower bound example. An unknot polygon with eight 2-sections. (G) A trefoil pattern enclosed in a 7-block which, when inserted at either of the 2-sections indicated by arrows, yields a trefoil polygon in  $\mathbb{T}^*$ . Note that the trefoil pattern could be modified at its ends to be inserted at any of the other 2-sections of the original polygon.

can occur in  $\mathbb{T}^*$  since they are all 4-plats. The family of 4-plats includes all twist knots and the T(2,n) torus links—knot and link types that are often observed in DNA experiments [52].

To prove the KE Conjecture for polygons in  $\mathbb{T}^*$ , we prove upper and lower bounds on  $p_{\mathbb{T}^*,n}(K)$  of the form in (1), differing only by a constant factor. We also establish similar results for non-split links with two or more components in  $\mathbb{T}^*$ . Since a knot is a 1-component non-split link, from here on we will only distinguish between knots and multi-component non-split links if necessary, or to connect to the KE Conjecture. The main result is as follows.

**Theorem 1.** Let L be any non-split link embeddable in the  $2 \times 1$  tube  $\mathbb{T}^*$ . There exist positive constants  $\epsilon \in (0,1), b_L \in \mathbb{R}, d_L \in \mathbb{Z}, e_L \in \mathbb{Z}$  (independent of n) and an integer  $N_{L,\epsilon} > 0$  such that for any  $n \geqslant N_{L,\epsilon}$ , there are bounds on  $p_{\mathbb{T}^*,n}(L)$  as follows:

$$\frac{1}{2} \binom{\lfloor \epsilon (n - e_L) \rfloor}{f_L} p_{\mathbb{T}^*, n - e_L}(0_1) \leqslant p_{\mathbb{T}^*, n}(L) \leqslant b_L \binom{n}{f_L} p_{\mathbb{T}^*, n + d_L}(0_1), \tag{3}$$

where  $f_L$  is the number of prime link factors in L. Also, there exist  $C_1$ ,  $C_2 > 0$  such that for all sufficiently large n

$$C_1 n^{f_L} p_{\mathbb{T}^*,n}(0_1) \leqslant p_{\mathbb{T}^*,n}(L) \leqslant C_2 n^{f_L} p_{\mathbb{T}^*,n}(0_1).$$
 (4)



When L=K is a knot embeddable in  $\mathbb{T}^*$ , (4) gives (1) of the KE Conjecture, up to the term  $B_K$ . More generally, for any link L, the bounds of theorem 1 establish these important consequences: the exponential growth constant for embeddings of L in  $\mathbb{T}^*$  is the same as that for unknot polygons (as in (2) of the KE Conjecture), and the entropic critical exponent increases by one for each prime factor of L. The latter assumes that the unknot entropic exponent  $\alpha_{\mathbb{T}^*,0_1}$  exists. Regarding (2), the exponential growth constant,  $\mu_{\mathbb{T}^*,0_1} = \lim_{n\to\infty} (p_{\mathbb{T}^*,n}(0_1))^{1/n}$ , for unknot polygons in  $\mathbb{T}^*$  is known to exist and the FWD conjecture holds [44]. The existence of  $\alpha_{\mathbb{T}^*,0_1}$  remains an open problem, however there is strong numerical evidence that  $\alpha_{\mathbb{T}^*,0_1} = 0$  [8, 23].

Our results about the exponential growth constants and entropic critical exponents for lattice polygons with fixed knot-type are believed to hold for any tube size [8, 23], as well as in the limit where the tube dimensions go to infinity (see [37, 42]). This is the first model for which they are proven. For multi-component non-split links, the growth constant result is known for embeddings in  $\mathbb{Z}^3$  of links with only unknot components [46]. Theorem 1 for  $\mathbb{T}^*$  yields the first results on the growth constants for all multi-component non-split links, and for how the entropic exponent changes with the link-type. Numerical evidence for multi-component non-split link embeddings in  $\mathbb{Z}^3$  suggests that the results in theorem 1 also hold for the unconfined case [10].

This letter is devoted to outlining the proof of theorem 1 and its connection to the KE conjecture. The bounds in theorem 1 (3) are each obtained by considering ways to convert an embedding of one link-type into an embedding of another link-type by insertions of sub-embeddings. The mathematical challenges and approaches for the upper bound are quite distinct from those for the lower bound. For the upper bound, the goal is to convert a non-trivial link L in  $\mathbb{T}^*$  to an unknot polygon as indicated in figures 2(A)–(E). The mathematical challenge for the upper bound is finding appropriate sub-embeddings (braid blocks) to insert at specific insertion locations in order to simplify the link. We solve this by using the classification of 4-plats [11, 43] and by proving new results about 4-plat diagrams (see theorem 3). For the lower bound, the goal is to convert an unknot polygon to an embedding of a non-trivial link L, as indicated by the insertion in figures 2(F) and (G). A known result [6], given here in proposition 2, provides suitable candidate sub-embeddings, called *link patterns*, which can be inserted at predefined locations (2-sections) to obtain an embedding of L. However, the lower bounds of (3) and (4) require that not only it be possible to insert the suitable link patterns, but that on average there must be many locations (i.e. O(n)) where this can be done. In theorem 5 we prove this result by establishing a *pattern theorem* for unknot polygons in  $\mathbb{T}^*$ .

The braid blocks and link patterns needed for the upper and lower bound arguments respectively are each different types of lattice link blocks, where a *block* is a piece of a lattice link between two half-integer constant *x*-planes. The *span* of a lattice link or any associated block is the absolute difference between its smallest and largest *x*-coordinates. An *s*-block is a block with span *s*. We say a lattice link has a *j*-section at a half-integer *x*-plane if the plane intersects exactly *j* edges of the lattice link.

Additional definitions and an overview of the upper and lower bound arguments leading to (3) of theorem 1 are given in sections 2 and 3, respectively. Arguments needed to obtain (4) of theorem 1, consequences related to the size of the linked region and the broader impact of all these results are discussed in section 4. We also discuss the challenges to extending the arguments to larger tubes. Detailed proofs will be published separately [9].



### 2. Upper bound in theorem 1: new knot theory and unknotting by braid-block insertion

To establish the *upper bound* (3) of theorem 1, in this section we outline how to transition between an embedding of a non-split link L in  $\mathbb{T}^*$  and a corresponding set of 4-plat diagrams, one for each prime factor of L. The ultimate goal is to 'unknot' the embedding by a sequence of  $f_L$  insertions of braid blocks, where a *braid block* (*braid s-block*) is defined to be a block (*s*-block) that corresponds to a 4-braid. This goal is achieved via the following theorem.

**Theorem 2.** Any lattice embedding of a non-split link L in  $\mathbb{T}^*$  can be converted to a lattice polygon of the unknot in  $\mathbb{T}^*$  by  $f_L$  insertions of braid s-blocks. The span (s) is bounded above by 3c + 8, where c is the maximum crossing number of the prime factors of L.

The *crossing number* of a link L is a topological invariant given by the minimal number of crossings over all its diagrams. Importantly, the span s of the braid blocks in theorem 2 is determined by the crossing numbers of the prime factors of L and does not depend on the size of the lattice embedding of L. Figure 2(A) illustrates the theorem for a trefoil (crossing number 3) polygon in  $\mathbb{T}^*$  with n = 98 edges, along with an embedding of a braid 3-block (figure 2(E)) that, upon insertion at the identified location, converts the trefoil to an unknot polygon.

From theorem 2, the upper bound (3) of theorem 1 is obtained as follows. Using theorem 2, we can insert a finite number of braid s-blocks to change an embedding of L into an unknot polygon. Then  $p_{\mathbb{T}^*,n}(L) \leq \binom{n+d_L}{f_L}p_{\mathbb{T}^*,n+d_L}(0_1)$ , where  $d_L$  is a fixed number (the total number of edges in the inserted parts) that is bounded above by a finite multiple of  $f_L$ . The binomial term in the upper bound accounts for the number of ways different embeddings of L could lead to the same unknot polygon; this is bounded above by the number of places (polygon edges) the inserted  $f_L$  braid blocks could be located in the unknot polygon, namely  $\binom{n+d_L}{f_L}$ . We then have  $\binom{n+d_L}{f_L} \leq b_L\binom{n}{f_L}$  for any constant  $b_L > 1$ , for n sufficiently large.

To establish theorem 2, we obtain several intermediate results. We establish a way to go between embeddings in  $\mathbb{T}^*$  and 4-plat diagrams. This first involves obtaining a *shifted diagram* from the embedding, as described in [28, Definition 3] and illustrated in figure 2(B). We also establish how to convert a 4-plat diagram of a link L into a diagram of the unknot by inserting a braid word (theorem 3 below). We then use arguments as in [28] to construct an s-block corresponding to any 4-braid word. Finally, the proof of theorem 3 indicates where to insert the s-blocks and unknot an embedding of L in  $\mathbb{T}^*$ . The proofs are outlined next.

A 4-braid can be defined as four disjoint strings in a rectangular cuboid, where the strings start at four points in the left (x=0) face of the cuboid and end at four points in the opposite (right) face. Each string is required to run strictly rightwards, i.e. for any c the string meets the plane x=c at most once. The 4-braid is studied using a 4-braid diagram obtained by projecting the braid onto the xy-plane and resolving over and under crossings. A 4-braid diagram with no crossings is said to be trivial. Any 4-braid, except the trivial one, can be obtained by joining elementary braids  $\sigma_1, \sigma_2, \sigma_3, \sigma_1^{-1}, \sigma_2^{-1}$  and  $\sigma_3^{-1}$  (see figure 3). A sequence of the letters  $\sigma_i^{\pm 1}$ , called a 4-braid word, represents a 4-braid and its corresponding 4-braid diagram. The empty word with no letters represents the trivial braid. The sequence of letters used for a braid word is written in simple exponential form, e.g.  $\sigma_i^a$  or  $\sigma_i^{-a}$ . Two 4-braids are equivalent if they are related by 'level preserving' isotopies, but they may be represented by different 4-braid diagrams and braid words. In particular, we consider that a reducible word,  $\sigma_i^a \sigma_i^{-b}$  or  $\sigma_i^{-b} \sigma_i^a$  ( $a, b \in \mathbb{N}$ ), is different from the reduced one,  $\sigma_i^{a-b}$ .

Given a 4-braid word w, its reverse word  $\overline{w}$  is obtained by reversing the order of the elementary braids in w. The inverse word  $w^{-1}$  of w is obtained by reversing the order of letters



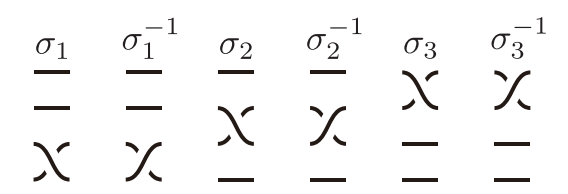
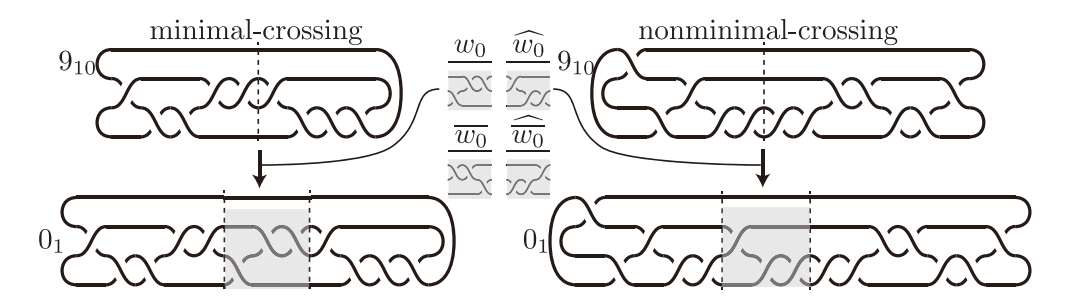


Figure 3. Elementary braids.



**Figure 4.** Insertions of  $w_0 = \sigma_1 \sigma_2^2$  and  $\widehat{w_0} = \sigma_2 \sigma_1^2$  on 4-plat diagrams for the 9 crossing 4-plat  $9_{10}$ . Unknot diagrams are obtained by these insertions.

and interchanging  $\sigma_i$  and  $\sigma_i^{-1}$ . For example,  $(\sigma_1 \sigma_2 \sigma_3^{-2})^{-1} = \sigma_3^2 \sigma_2^{-1} \sigma_1^{-1}$ . Note that the words  $ww^{-1}$  and  $w^{-1}w$  represent braids that are equivalent to the trivial braid. By convention, a 4-braid word that does not contain any  $\sigma_3^{\pm 1}$  is called a 3-braid word since one string in the braid diagram has no crossings. The *flipped word*  $\widehat{w}$  of a 3-braid word w is obtained by interchanging the 1's and 2's in the subscripts of the elementary braids in w.

To prove theorem 2 we establish that any 4-plat diagram can be changed into a diagram of the unknot by inserting a specific 4-braid.

**Theorem 3.** For any 4-plat L, there exists a 3-braid word  $w_0$  such that any given 4-plat diagram of L can be converted into a diagram of the unknot by inserting one of  $w_0, \overline{w_0}, \widehat{w_0}$  and  $\overline{w_0}$ . Moreover,  $w_0$  can be taken so that the number of crossings of  $w_0$  is at most the crossing number of L.

In the case of the knot  $9_{10}$ ,  $w_0 = \sigma_1 \sigma_2^2$  satisfies the condition in theorem 3. Namely, any given 4-plat diagram of  $9_{10}$  can be converted into a diagram of the unknot by inserting either  $w_0 = \sigma_1 \sigma_2^2$ ,  $\overline{w_0} = \sigma_2^2 \sigma_1$ ,  $\widehat{w_0} = \sigma_2 \sigma_1^2$  or  $\widehat{\overline{w_0}} = \sigma_1^2 \sigma_2$ . See figure 4. For a given link type L, there can be many options for  $w_0$ .

A key element of the proof of theorem 3 is the definition of seven types of 4-plat diagram moves, and the proof that they preserve link-type. We then focus on a minimal-crossing 4-plat diagram,  $D_0$ , of L and find an inserting 3-braid word  $w_0$  of theorem 3. There is always one choice for  $w_0$  that can be obtained from the inverse word for  $D_0$  (with its length bounded by the number of crossings in L), however, shorter choices can exist as in figure 4.

The remaining proof of theorem 3 consists of showing that the cases for all other (minimal and non minimal-crossing) 4-plat diagrams D can be handled by deforming them to  $D_0$  using 4-plat diagram moves that reduce or preserve the crossing number. We get the following theorem.

**Theorem 4.** Suppose D and  $D_0$  are 4-plat diagrams of L, and  $D_0$  is a minimal-crossing diagram. If a link K is obtained by inserting a 3-braid word  $w_0$  into  $D_0$ , then K can be obtained from D by inserting one of  $w_0, \overline{w_0}, \widehat{w_0}$  and  $\widehat{\widehat{w_0}}$ .



Theorem 3 is obtained by taking *K* to be the unknot in theorem 4. The following proposition allows us to connect theorem 3 to theorem 2.

**Proposition 1.** Let  $w_0$  be a 3-braid word with c crossings. There is a span-3c braid block in  $\mathbb{T}^*$  representing  $w_0$ . Moreover, for each type of 4-section there is a braid block in  $\mathbb{T}^*$  with span at most 3c + 8 that represents  $w_0$  and can be inserted into the 4-section.

The proof of proposition 1 is constructive and uses similar arguments to those of [28]. This proposition allows us to connect theorem 3 to theorem 2 provided that we are able to associate 4-plat diagrams to lattice embeddings. For the latter, we determine sufficient conditions for the shifted diagram of an embedding of prime link L in  $\mathbb{T}^*$  to be a 4-plat diagram. We then show that we can divide an embedding of any link L into a sequence of separate link embeddings, one for each prime factor of L, and each with an associated 4-plat diagram. The resulting diagrams allow for the direct identification of the insertion points for the braid blocks of proposition 1 into the original embedding of L.

## 3. Lower bound in theorem 1: a pattern theorem for unknots in $\mathbb{T}^*$ and link pattern insertion

We start with some definitions and review of known results. A *connected sum pattern* is a lattice link block that starts and ends at a 2-section. Such a pattern is called a *link pattern* if closing off each end of the pattern yields a non-trivial non-split link. Otherwise it is called an *unknot pattern*. See figure 2(G) for an example of a link pattern for a  $3_1$  knot in  $\mathbb{T}^*$  with span 7. By definition, if a lattice embedding of L has a link pattern, then the corresponding link type is a connected summand of L. Arguments in [6] establish the following results for any  $\mathbb{T}$ .

**Proposition 2 ([6, result 4]).** For each link L embeddable in  $\mathbb{T}$ , there is a link-pattern of L.

Figures 2(F) and (G) illustrate how a  $3_1$  link pattern can be inserted at a 2-section of an unknot polygon to form a  $3_1$  polygon. An unknot polygon with at least one 2-section can be decomposed into the connected sum of two unknots, allowing for the 'insertion' of any link pattern (see figure 2(G)).

**Proposition 3 ([28, corollary 2]).** If a link type L can be embedded in  $\mathbb{T}^*$  then each prime factor of L is a 4-plat. Furthermore, there is an embedding of L in  $\mathbb{T}^*$  which consists of a connected sum of  $f_L$  link-patterns, one corresponding to each prime factor of L.

**Corollary 1.** Consider a link L embeddable in  $\mathbb{T}^*$ . Any unknot polygon with at least one 2-section can be converted to an embedding of L by  $f_L$  insertions of link-patterns at one or more of the 2-sections of the polygon.

For the lower bound of (3) in theorem 1, we need to know that most unknot polygons contain a sufficient number of 2-sections. We do this by establishing a *pattern theorem* for unknot polygons using information from exact transfer-matrix calculations for polygons in the tube  $\mathbb{T}^*$ . In essence, a pattern theorem is a result stating that a particular type of lattice object (polygon, walk, tree, etc), as its size n gets large, typically contains many copies of a small piece (a *pattern*).

Pattern theorems have been used previously, for example, to prove the FWD conjecture for polygons in tubes [4, 44] and to study linking probabilities for the case of two polygons which span a tube [3]. Theorem 5 below can be understood as a pattern theorem for unknot polygons in  $\mathbb{T}^*$ . In particular this theorem establishes that for n sufficiently large, all but exponentially



few *n*-edge unknot polygons (unknots in  $\mathbb{T}^*$ ) contain a density  $(\epsilon n)$  of 2-sections. Since an unknot pattern can be inserted at any of these 2-sections, a pattern theorem results.

**Theorem 5.** Let  $p_{\mathbb{T}^*,n}(0_1,\leqslant k)$  be the number of unknots of length n in  $\mathbb{T}^*$  which contain at most k 2-sections. Then there exists an  $\epsilon > 0$  such that

$$\limsup_{n \to \infty} \frac{1}{n} \log p_{\mathbb{T}^*, n} \left( 0_1, \leqslant \epsilon n \right) < \log \mu_{\mathbb{T}^*, 0_1}, \tag{5}$$

where n is even and  $\mu_{\mathbb{T}^*,0}$ , is the unknot growth constant.

Theorem 5 is key to establishing the lower bound of (3). For this, consider L a prime link. Let P be a connected sum pattern for L and let S be any 2-section. Then from corollary 1, P can be inserted (additional edges may be needed) at S in a polygon (see for example figure 2(G)), increasing the length of the resulting embedding by some constant  $\Delta$  depending on P (but not S).

Now take any unknot polygon with n edges and at least  $\epsilon n$  2-sections, with  $\epsilon$  the same as in theorem 5. By the above, the pattern P can be inserted at any one of those 2-sections, and the resulting lattice embedding will have link type L. We thus have

$$\binom{\epsilon n}{1} \left[ p_{\mathbb{T}^*,n}(0_1) - p_{\mathbb{T}^*,n}(0_1, \leqslant \epsilon n) \right] \leqslant p_{\mathbb{T}^*,n+\Delta}(L). \tag{6}$$

However, from theorem 5 we have

$$\lim_{n \to \infty} \frac{p_{\mathbb{T}^*,n}(0_1) - p_{\mathbb{T}^*,n}(0_1, \leqslant \epsilon n)}{p_{\mathbb{T}^*,n}(0_1)} = 1$$
 (7)

so that the numerator can be made arbitrarily close to the denominator for sufficiently large n. Hence, for example, there exists N > 0 such that for all  $n \ge N$ ,  $\frac{1}{2} \binom{\epsilon n}{1} p_{\mathbb{T}^*,n}(0_1) \le p_{\mathbb{T}^*,n+\Delta}(L)$ .

This argument can be extended in a straightforward way to the case where L is composite (see corollary 1) and the lower bound of (3) follows. Furthermore, taking  $L = 0_1$  in the above argument implies that all but exponentially few *n*-edge unknots in  $\mathbb{T}^*$  contain a density of any given unknot pattern, and hence the first proof of a pattern theorem for unknot polygons

As outlined below, we prove theorem 5 by establishing two intermediate results and then combining them.

### • Unknots with no 2-sections are exponentially rare:

Define  $p_{\mathbb{T}^*,n}$  to be the total (regardless of knot-type) number of *n*-edge polygons in  $\mathbb{T}^*$  with at least one edge in the plane x = 0. It will be convenient to refer to logarithms of growth constants. Given any growth constant such as  $\mu_{\mathbb{T}^*} = \lim_{n \to \infty} (p_{\mathbb{T}^*,n})^{1/n}$  or  $\mu_{\mathbb{T}^*,0}$ , we define a corresponding growth rate,  $\kappa_{\mathbb{T}^*} \equiv \log \mu_{\mathbb{T}^*}$  or  $\kappa_{\mathbb{T}^*}(0_1) \equiv \log \mu_{\mathbb{T}^*,0_1}$ .

The key result here is that

$$\hat{\kappa}_{\mathbb{T}^*}\left(0_1\right) < \kappa_{\mathbb{T}^*}\left(0_1\right),\tag{8}$$

where  $\hat{\kappa}_{\mathbb{T}^*}(0_1)$  (respectively  $\hat{\kappa}_{\mathbb{T}^*}$ ) is the growth rate of unknot polygons (respectively all polygons) with no 2-sections. We show this by computationally proving two inequalities:  $\hat{\kappa}_{\mathbb{T}^*} < 0.446287$  and  $\kappa_{\mathbb{T}^*}(0_1) \geqslant 0.620044$ . The first of these follows by computing the transfer matrix for polygons with no 2-sections and then deriving a bound on its spectral radius; the second follows by computing the number of unknots of length 24 in  $\mathbb{T}^*$  (which happens to be 119 796 593) and then using this to derive a lower bound on the growth rate.



• 2-sections can be removed from unknots: The main result here is that there exists a positive constant E such that

$$p_{\mathbb{T}^*,n}(0_1, \leqslant k) = \sum_{t=0}^k p_{\mathbb{T}^*,n}(0_1, t) \leqslant \sum_{t=0}^k 2^t \binom{\frac{n}{2}}{t} p_{\mathbb{T}^*,n+E_t}(0_1, 0). \tag{9}$$

This follows by taking any unknot polygon with t 2-sections, breaking it apart at each 2-section, and then joining all the pieces back together in a way that results in an unknot polygon with no 2-sections and Et more edges. The factor  $2^t {\frac{g}{t}}$  accounts for possible ambiguity when reversing the process.

Combining (8) and (9) to prove theorem 5:
 Equation (5) of theorem 5 essentially follows by setting k = εn in (9) and taking n → ∞.
 Using Stirling's approximation this gives

$$\limsup_{n\to\infty}\frac{1}{n}\log p_{\mathbb{T}^*,n}\left(0_1,\leqslant\epsilon n\right)\leqslant -\epsilon\log\epsilon-\left(\frac{1}{2}-\epsilon\right)\log\left(1-2\epsilon\right)+\left(1+\epsilon E\right)\hat{\kappa}_{\mathbb{T}^*}\left(0_1\right). \tag{10}$$

The bound (8) is then used as a bound on the right hand side for  $\epsilon > 0$  small.

### 4. Consequences and discussion

In this section we highlight some of the consequences of theorem 1 and its proof and present a general discussion of the results.

First, the arguments in sections 2 and 3 establish (3) of theorem 1. (4) can be obtained from (3) by combining the well-known fact that  $\lim_{n\to\infty} \frac{\log\binom{n}{b}}{\log n} = b$  with a new ratio limit result:

$$\lim_{n \to \infty} \frac{p_{\mathbb{T}^*, n+m}(0_1)}{p_{\mathbb{T}^*, n}(0_1)} = (\mu_{\mathbb{T}^*, 0_1})^m, \tag{11}$$

for any given even  $m \ge 2$ . The ratio limit (11) follows from the pattern theorem for unknot polygons and arguments from [31].

More generally, combining arguments similar to those for lattice clusters in [31] with the results of theorem 1 yields a general pattern theorem for the occurrence of unknot patterns in embeddings of any non-split link L. This pattern theorem and the proof of theorem 1 provide several ways to clarify the connection between the knot entropy results and the localization of knots in polymers.

To measure knot/link localization, a measure of the size (number of edges) of the entangled region and its comparison to the size of the whole embedding are needed. Several different approaches have been suggested for defining the size of the knotted region in polygons (e.g. [33]). A natural definition of this size for an n-edge embedding E with link-type E in a tube is as follows [6]. First divide E at each 2-section to create a set of patterns which can each be closed off into embeddings of links. Up to f of the resulting embeddings will be non-trivial links and the sizes of these non-trivial pieces can be summed to give the *size* of the linked part of E. To talk about how localized the linked part is, one considers a set of E of the size of the linked part is E of the linked part is said to be 'not localized'. Further, if the size of the linked part is E of the linked part is E of the linked part is one considers how the average size of the linked part is E of the linked part is said to be 'not localized'. Further, if the size of the linked part is E of the linked part is one considers how the average size of the linked part is E of the linked part is one considers how the average size of the linked part is E of the linked part is one considers how the average size of the linked part is E of the linked part is one considers have E of the linked part is one considers have E of the linked part is one considers have E of the linked part is one considers have E of the linked part is one considers have E of the linked part is one considers have E of the linked part is one considers have E of the linked part is one considers have E of the linked part is one considers have E of the linked part is one considers have E of the linked part is one considers have E of the linked part is one considers have E of the linked part is one considers have E of the linked part is one considers ha



The general pattern theorem for embeddings of a non-split link L implies that all but exponentially few n-edge embeddings of L contain a density  $(\epsilon n)$  of 2-sections. Dividing an embedding with  $\epsilon n$  2-sections into connected sum patterns, yields patterns with average size  $1/\epsilon$ . Thus one expects the link patterns in this to have, on average, a similar size and hence be O(1), i.e. strongly localized. Also, the upper bound proof of theorem 1 establishes that one can unknot a link by the insertion of  $f_L$  O(1)-size braid blocks. Therefore, in some sense the 'essential' parts of the link can be removed by making O(1) changes, another indication of strong localization. Other connections between theorem 1 and knot localization will be explored in a separate publication.

It is expected that bounds of the form in theorem 1 (4) hold for any tube size and in the limit as the tube dimensions go to infinity, i.e. for  $\mathbb{Z}^3$  [10, 37, 42]. Since (by arguments analogous to those in [27, 47])  $\mu_{0_1} = \lim_{M \to \infty} \mu_{\mathbb{T}_{M,M},0_1}$ , proof of such bounds for arbitrary tubes could lead to results for the unconfined case. Here we have outlined new strategies for both the upper and lower bound results. Although these strategies do not immediately generalize to all tube sizes, they provide promising new directions. Our proofs also identify some fundamental mathematical challenges that remain. For example, the upper bound arguments do not easily extend to a 3 × 1 tube since the extra configurational freedom means that obtaining a 4-plat diagram from an embedding of a 4-plat link will require additional combinatorial analysis. For the lower bound, the challenge for extending to larger tubes is two-fold, both limited by available computational resources. Firstly, the transfer-matrix for polygons in the tube would be needed (these have been computed for tube sizes up to 5 × 1 and 3 × 2 [23]). Secondly, an accurate count of unknot polygons up to a sufficiently large size is needed; in general this involves generating polygons and checking their knot-type.

Modelling knotting and linking in tubes is of independent interest to scientists working at the interface of polymer science and molecular biology. Recent experimental studies report on the detection of complex DNA knots using nanopore sensors [30, 41]. These methods allow researchers to detect knotting at length scales one order of magnitude larger than traditional gel electrophoresis [49, 53], where the limit on knot and link type detection is in the  $10^3$  base pair range [12, 14, 15, 26]. Experimental results have sparked interest in computational modelling of DNA knot translocation through narrow channels (e.g. [50]; reviewed in [38]). The  $2 \times 1$  tube studied here gives a theoretical framework to study knotting and linking in narrow channels. Our results provide a robust theoretical justification that knots and links confined to narrow tubular regions tend on average to have the entanglements localized and separated from each other in the tube. Indeed, the results for  $\mathbb{T}^*$  establish that knot factors occur as though they were distributed binomially along an unknot polygon; this is consistent with the Poisson distribution observed for a variety of tube sizes in the off-lattice model of [34].

### Data availability statement

The data cannot be made publicly available upon publication because they are not available in a format that is sufficiently accessible or reusable by other researchers. The data that support the findings of this study are available upon reasonable request from the authors.

### **Acknowledgments**

N R B was supported by Australian Research Council Grants DE170100186 and DP230100674. K I was supported by Japan Society for the Promotion of Science (JSPS) KAKENHI Grant Numbers JP17K14190, JP23K03114. K S is partially supported by Japan



Society for the Promotion of Science (JSPS) KAKENHI Grant Numbers JP16H03928, JP16K13751, JP19K21827, JP21H00978, JP23K20791. C E S acknowledges the support of the Natural Sciences and Engineering Research Council of Canada (NSERC), [funding reference number RGPIN-2020-06339], as well as Compute Canada resource allocations and past CRG support from the Pacific Institute for the Mathematical Sciences (PIMS). M V was supported by the National Science Foundation (NSF) Division of Mathematical Sciences (DMS) Grants 1817156 and 2054347.

#### **ORCID iDs**

Nicholas R Beaton https://orcid.org/0000-0001-8220-3917 Kai Ishihara https://orcid.org/0000-0001-5994-0265 Mahshid Atapour https://orcid.org/0000-0002-5385-2667 Jeremy W Eng https://orcid.org/0000-0002-2006-017X Mariel Vazquez https://orcid.org/0000-0001-8328-6806 Koya Shimokawa https://orcid.org/0000-0001-7196-9060 Christine E Soteros https://orcid.org/0000-0003-3682-7440

#### References

- [1] Alm S E and Janson S 1990 Random self-avoiding walks on one-dimensional lattices Commun. Stat. Stoch. Models 6 169–212
- [2] Arsuaga J, Vazquez M, McGuirk P, Trigueros S, Sumners D W and Roca J 2005 DNA knots reveal a chiral organization of DNA in phage capsids *Proc. Natl Acad. Sci.* 102 9165–9
- [3] Atapour M, Soteros C E, Ernst C and Whittington S G 2010 The linking probability for 2component links which span a lattice tube J. Knot Theory Ramif. 19 27–54
- [4] Atapour M, Soteros C E and Whittington S G 2009 Stretched polygons in a lattice tube *J. Phys. A: Math. Theor.* **42** 322002
- [5] Atapour M 2008 Topological entanglement complexity of systems of polygons and walks in tubes PhD Dissertation University of Saskatchewan, Saskatoon, Canada
- [6] Beaton N R, Eng J W, Ishihara K, Shimokawa K and Soteros C E 2018 Characterising knotting properties of polymers in nanochannels Soft Matter 14 5775–85
- [7] Beaton N R, Eng J W and Soteros C E 2016 Polygons in restricted geometries subjected to infinite forces J. Phys. A: Math. Theor. 49 424002
- [8] Beaton N R, Eng J W and Soteros C E 2019 Knotting statistics for polygons in lattice tubes J. Phys. A: Math. Theor. 52 144003
- [9] Beaton N R, Ishihara K, Atapour M, Eng J W, Vazquez M, Shimokawa K and Soteros C E 2023 Entanglement statistics of polymers in a lattice tube and unknotting of 4-plats (arXiv:2204.06186)
- [10] Bonato A, Orlandini E and Whittington S G 2021 Asymptotics of multicomponent linked polygons J. Phys. A: Math. Theor. 54 235002
- [11] Burde G, Zieschang H and Heusener M 2014 Knots (De Gruyter Studies in Mathematics vol 5) 3rd edn (De Gruyter)
- [12] Cebrián J et al 2014 Electrophoretic mobility of supercoiled, catenated and knotted DNA molecules Nucleic Acids Res. 43 e24
- [13] Chapman H and Rechnitzer A 2019 A Markov chain sampler for plane curves Exp. Math. 31 552–82
- [14] Crisona N J, Weinberg R L, Peter B J, Sumners D W and Cozzarelli N R 1999 The topological mechanism of phage λ integrase J. Mol. Biol. 289 747–75
- [15] Crisona N J, Kanaar R, Gonzalez T N, Zechiedrich E, Klippel A and Cozzarelli N R 1994 Processive recombination by wild-type Gin and an enhancer-independent mutant J. Mol. Biol. 243 437–57
- [16] Dai L, van der Maarel J and Doyle P S 2014 Extended de Gennes regime of DNA confined in a nanochannel Macromolecules 47 2445–50
- [17] Delbrück M and Fuller F B 1962 Mathematical problems in the biological sciences *Proc. Symp. on Applied Mathematics* vol 14 (American Mathematical Society) pp 55–63



- [18] Diao Y, Ernst C, Montemayor A, Rawdon E and Ziegler U 2014 The knot spectrum of confined random equilateral polygons *Comput. Math. Biophys.* 2 19–33
- [19] Diao Y, Nardo J C and Sun Y 2001 Global knotting in equilateral random polygons J. Knot Theory Ramif. 10 597–607
- [20] Diao Y 1995 The knotting of equilateral polygons in  $\mathbb{R}^3$  J. Knot Theory Ramif. **04** 189–96
- [21] Diao Y, Pippenger N and Sumners D W 1994 On random knots J. Knot Theory Ramif. 03 419–29
- [22] Eng J W 2014 Self-avoiding polygons in (*L*, *M*)-tubes *Master's Thesis* University of Saskatchewan, Saskatoon, Canada
- [23] Eng J W 2020 A transfer matrix approach to studying the entanglement complexity of self-avoiding polygons in lattice tubes *PhD Dissertation* University of Saskatchewan, Saskatoon, Canada
- [24] Even-Zohar C, Hass J, Linial N and Nowik T 2018 The distribution of knots in the Petaluma model Algebr. Geom. Topol. 18 3647–67
- [25] Frisch H L and Wasserman E 1961 Chemical topology J. Am. Chem. Soc. 83 3789–95
- [26] Grainge I, Bregu M, Vazquez M, Sivanathan V, Ip S C Y and Sherratt D J 2007 Unlinking chromosome catenanes in vivo by site-specific recombination EMBO J. 26 4228–38
- [27] Hammersley J and Whittington S 1985 Self-avoiding walks in wedges J. Phys. A: Math. Gen. 18 101
- [28] Ishihara K, Pouokam M, Suzuki A, Scharein R, Vazquez M, Arsuaga J and Shimokawa K 2017 Bounds for minimum step number of knots confined to tubes in the simple cubic lattice J. Phys. A: Math. Theor. 50 215601
- [29] Jungreis D 1994 Gaussian random polygons are globally knotted J. Knot Theory Ramif. 03 455–64
- [30] Kumar Sharma R, Agrawal I, Dai L, Doyle P S and Garaj S 2019 Complex DNA knots detected with a nanopore sensor *Nat. Commun.* 10 4473
- [31] Madras N 1999 A pattern theorem for lattice clusters Ann. Comb. 3 357-84
- [32] McClintock B 1932 A correlation of ring-shaped chromosomes with variegation in Zea mays Proc. Natl Acad. Sci. USA 18 677–81
- [33] Micheletti C, Marenduzzo D and Orlandini E 2011 Polymers with spatial or topological constraints: theoretical and computational results *Phys. Rep.* **504** 1–73
- [34] Micheletti C and Orlandini E 2012 Knotting and metric scaling properties of DNA confined in nano-channels: a Monte Carlo study Soft Matter 8 10959–68
- [35] Navashin M S 1930 Studies on Polyploidy: Cytological Investigations on Triploidy in Crepis (University of California Publications in Agricultural Sciences vol 1) (University of California Press) pp 95–106
- [36] Orlandini E, Tesi M C, Janse van Rensburg E J and Whittington S G 1996 Entropic exponents of lattice polygons with specified knot type J. Phys. A: Math. Gen. 29 L299
- [37] Orlandini E, Tesi M C, Janse van Rensburg E J and Whittington S G 1998 Asymptotics of knotted lattice polygons J. Phys. A: Math. Gen. 31 5953–67
- [38] Orlandini E and Micheletti C 2021 Topological and physical links in soft matter systems *J. Phys.:* Condens. Matter 34 013002
- [39] Orlandini E, Stella A L and Vanderzande C 2009 The size of knots in polymers Phys. Biol. 6 025012
- [40] Pippenger N 1989 Knots in random walks Discrete Appl. Math. 25 273-8
- [41] Plesa C, Verschueren D, Pud S, van der Torre J, Ruitenberg J W, Witteveen M J, Jonsson M P, Grosberg A Y, Rabin Y and Dekker C 2016 Direct observation of DNA knots using a solid-state nanopore *Nat. Nanotechnol.* 11 1093–7
- [42] Janse van Rensburg E J and Rechnitzer A 2011 On the universality of knot probability ratios J. Phys. A: Math. Theor. 44 162002
- [43] Schubert H 1956 Knoten mit zwei Brücken Math. Z. 65 133-70
- [44] Soteros C E 1998 Knots in graphs in subsets of  $\mathbb{Z}^3$  Topology and Geometry in Polymer Science (The IMA Volumes in Mathematics and its Applications vol 103) (Springer) pp 101–33
- [45] Soteros C E 2006 Eulerian graph embeddings and trails confined to lattice tubes J. Phys.: Conf. Ser. 42 258–67
- [46] Soteros C E, Sumners D W and Whittington S G 1999 Linking of random p-spheres in  $\mathbb{Z}^d$  J. Knot Theory Ramif. 8 49–70
- [47] Soteros C E, Sumners D W and Whittington S G 2012 Knotted 2-spheres in tubes in Z<sup>4</sup> J. Knot Theory Ramif. 21 1250116
- [48] Soteros C E and Whittington S G 1989 Lattice models of branched polymers: effects of geometrical constraints J. Phys. A: Math. Gen. 22 5259–70
- [49] Stasiak A, Katritch V, Bednar J, Michoud D and Dubochet J 1996 Electrophoretic mobility of DNA knots Nature 384 122–122



- [50] Suma A and Micheletti C 2017 Pore translocation of knotted DNA rings Proc. Natl Acad. Sci. 114 E2991–7
- [51] Sumners D W and Whittington S G 1988 Knots in self-avoiding walks J. Phys. A: Math. Gen. 21 1689
- [52] Sumners D W, Ernst C, Spengler S J and Cozzarelli N R 1995 Analysis of the mechanism of DNA recombination using tangles Q. Rev. Biophys. 28 253–313
- [53] Trigueros S, Arsuaga J, Vazquez M E, Sumners D W and Roca J 2001 Novel display of knotted DNA molecules by two-dimensional gel electrophoresis *Nucleic Acids Res.* 29 e67
- [54] Wall F T, Seitz W A, Chin J C and Gennes P G D 1978 Statistics of self-avoiding walks confined to strips and capillaries *Proc. Natl Acad. Sci.* 75 2069–70
- [55] Witte S L 2019 Link nomenclature, random grid diagrams, and Markov chain methods in knot theory *PhD Dissertation* University of California Davis, Davis, California